Reorganization of finger coordination patterns during adaptation to rotation and scaling of a newly learned sensorimotor transformation: Supplemental Information

Xiaolin Liu, Kristine M. Mosier, Ferdinando A. Mussa-Ivaldi, Maura Casadio and Robert A. Scheidt

1. Numerical Simulations

We performed a set of inverse dynamics analyses and forward dynamic numerical simulations of goal-directed reaching with the arm to: 1) explore patterns of kinetic coordination at the shoulder and elbow joints during a common reaching task, and 2) determine how these patterns change during compensation for an imposed visuomotor rotation or scaling. Eight standard template movements were created within the MATLAB computing environment (The Mathworks, Inc., Natick MA). These were straight-line reaching movements of 10 cm length and 0.5 s duration in the horizontal plane (Figs S1A and S1B, top). Movements originated from a position 0.4 m in front of the subject and 0.05 m to the left of the shoulder center of rotation. The movements were directed outward from this origin to eight targets equally distributed across directions in the horizontal plane. A movement to the subject's right was considered a 0° movement, with positive angles corresponding to counter-clockwise (CCW) deviations. An additional set of 'short' (0.05 m long) template movements was implemented from the same origin with the same 0.5 s duration.

The analysis was conducted in four stages. First, inverse kinematic calculations were performed to calculate shoulder and elbow joint excursions required to perform each template movement. The anthropometric parameters used for joint motions for a typical subject were based on previously published simulations of reaching and adaptation to velocity-dependent force fields (Shadmehr and Mussa-Ivaldi 1994) and were modified to attain a limb damping factor within the physiological range (cf. Perreault et al. 2004) (Table S1; see also Scheidt and Ghez, 2007).

Table S1: Anthropometric and joint mechanical properties used to simulate arm movements.

Parameter	Value
upper arm length	0.33 m
upper arm mass	2.62 kg
upper arm center of mass	0.165 m
upper arm inertia	0.0231 kg-m^2
forearm / hand length	0.34 m
forearm / hand mass	1.52 kg
forearm / hand center of mass	0.19 m
forearm / hand inertia	0.0372 kg-m^2
joint viscosity	$V = \begin{bmatrix} 2.1 & 0.8 \\ 0.8 & 2.2 \end{bmatrix}$ N-m-s/rad

Second, the shoulder (τ_s) and elbow (τ_e) joint torques required to drive the simulated limb through the template trajectories (i.e. the generalized muscle torques of Sainburg et al., 1995) were estimated using inverse dynamics equations of motion, expressed as:

$$\begin{bmatrix}\tau_s\\ \tau_e\end{bmatrix}=\begin{bmatrix}I_s+I_e+m_s r_s^2+m_e r_e^2+m_e l_s^2+2l_s m_e r_e\cos(\theta_e) & I_e+m_e r_e^2+l_s m_e r_e\cos(\theta_e)\\ I_e+m_e r_e^2+l_s m_e r_e\cos(\theta_e) & I_e+m_e r_e^2\end{bmatrix}\begin{bmatrix}\ddot{\theta}_s\\ \ddot{\theta}_e\end{bmatrix}$$
$$+\begin{bmatrix}0 & -l_s m_e r_e\sin(\theta_e) & -2l_s m_e r_e\sin(\theta_e)\\ l_s m_e r_e\sin(\theta_e) & 0 & 0\end{bmatrix}\begin{bmatrix}\dot{\theta}_s^2\\ \dot{\theta}_e^2\\ \dot{\theta}_s\dot{\theta}_e\end{bmatrix}+\begin{bmatrix}V_{11} & V_{12}\\ V_{21} & V_{22}\end{bmatrix}\begin{bmatrix}\dot{\theta}_s\\ \dot{\theta}_e\end{bmatrix} \quad [S1]$$

Here, the arm was modeled as a two-segment link in the horizontal plane (cf. Scheidt et al., 2005). Each segment was modeled as a homogeneous rigid body with mass $\boldsymbol{m_i}$, length $\boldsymbol{l_i}$, moment of inertia $\boldsymbol{I_i}$, and center of mass located at distance $\boldsymbol{r_i}$ from the proximal joint. $\boldsymbol{\theta_i}$ are the joint angles where the index $\boldsymbol{i = s}$ corresponds to the shoulder joint and $\boldsymbol{i = e}$ corresponds to the elbow joint. Because we were interested in kinetic coordination across joints, we ignored the possible influence of limb postural stabilization about the goal target at the end of movement (see Scheidt and Ghez, 2007, for an analysis of those effects in horizontal planar reaching). Note also that we make no assumption regarding how the nervous system produces generalized muscle torques, whether by modulating motor neuron threshold potentials as in equilibrium trajectory models or by simply specifying a time series of muscle activations. Both approaches yield the same feedforward joint torques in the absence of environmental perturbations (as is the case with the visuomotor perturbations studied in Krakauer et al., 2000).

Third, we compared coordination between joints within single movements by plotting elbow torque as a function of shoulder torque at each moment in time (eg. Fig S1C). We also compared how patterns of coordination within joints would have to change to compensate for either a 2x scaling of cursor motion relative to hand motion or a 45° counter-clockwise rotation of cursor motion about the common movement origin. We did so by plotting elbow and shoulder torques as a function of time for the standard template movements and their shortened (Fig S1D) or 45° clockwise-rotated versions (Fig S1E).

Finally, we conducted a set of forward dynamic simulations to evaluate the feasibility of altering the extent of straight-line hand movements by applying a common, direction-independent scaling factor to patterns of joint torques suited for moving to targets at a single, different distance. Movements were simulated by propagating the forward dynamic equations of motion forward in time (i.e. by solving Eq. S1 for θ at each moment in time), subject either to the torques calculated along the templates or to a scaled version of those torques. Because postural stabilization increases the restorative effects of limb visocelasticity about the desired target configuration (Lacquaniti et al., 1993; Gomi and Osu, 1998) and because the model of Eq. S1 ignores these effects, simulations based on Eq. S1 provides a worst-case analysis of the mechanical consequences of feedforward motor command planning errors introduced by application of a scaling factor to kinetic coordination patterns drawn from movements half the desired extent. We evaluated the sensitivity of simulation results to the particular values of effective joint viscosity specified in Table S1 by systematically varying matrix V over a ± 10-fold range in both the inverse- and forward-dynamics computations.

2. Results

We simulated movements with monotonic displacements (Fig S1B, trace d) and smooth hand speed profiles (Fig S1B, trace s). Inverse dynamic joint torque estimates for the three highlighted trajectories in panel A reveal that the two 0°

trajectories required similarly-shaped torque waveforms at both the shoulder and elbow joints, albeit with different magnitudes (Fig S1B, compare blue and black traces). In contrast, the torque waveforms needed to compensate for a CCW visuomotor rotation differed both in sign (elbow) and magnitude (shoulder) from those for the 0° baseline target (Fig S1B, compare red and black traces). These differences indicate that compensating for a rotation requires a dramatic change in the temporal phasing of inter-joint coordination (Fig S1C, compare black and red traces from the 0° and 315° trajectories, respectively) whereas compensating for a scaling of movement does not (Fig S1C, compare black and small dark blue traces). Importantly, by multiplying both of the shorter movement's joint torques by common scaling factor – the ratio of desired vs. original movement extents, or x2 in these simulated movements - the pattern of inter-joint coordination observed in the baseline trajectory is largely recovered. We obtain similar results when this same scaling relationship is applied to the short template movements in each of the other directions (Fig S1D).

It is not as easy to see how inter-joint coordination should be reorganized to induce a common rotation of point-to-point reaches. Compare, for example, traces a, b, and c in Fig S1E, which correspond to intended movements in the 45°, 135° and the 225° target directions. For both the 45° and 225° movements, elbow torque profiles were very similar before (black traces) and after (red traces) compensating for the visuomotor rotation. In contrast, shoulder torques oppositely directed and had different magnitude ratios before and after rotation in these two cases. For the 135° target direction, the pattern was reversed. Here, shoulder torques were similar before and after compensating for the rotation whereas the elbow torques differed in sign. In other directions (eg. 0°), other different patterns were observed. No simple scaling or staggering of joint torques can be commonly applied across movement directions to induce a common rotation of point-to-point reaches.

Results of the forward-dynamics simulations reveal that only small movement errors would be introduced by applying a common kinetic scaling rule across movement directions (Fig S1F, left). These errors result from neglecting extent-related differences in interaction torque magnitudes, which do not scale in direct proportion to the visuomotor scaling factor but rather scale as the square of this factor. The results of a sensitivity analysis on the effects of joint viscosity magnitude found that our findings were robust over a 100-fold range of V (Fig S1F, center and right).

3. Conclusions

This analysis has revealed a fundamental asymmetry in the dynamics of compensation for a visuomotor scaling and rotation: It is a simple matter to compensate for a visuomotor scaling because a single gain factor can be applied across joints and movement directions to adjust movement extent. The striking simplicity of this approximate scaling relationship derives from Newton's second law for rotational systems ($\tau = I\,\ddot{\theta}$), from the fact that the limb's mechanical response to application of muscle torque is largely dominated by the limb's inertia (i.e. the effects of interaction torques are modest in point-to-point reaching) and from the fact that the nonlinearities inherent to multi-joint limb motion are smooth. In contrast, the reorganization of inter-joint coordination needed to compensate a visuomotor rotation is complex and direction-dependent. An adaptive system capable to distinguish extent from direction errors could learn to capitalize on this inherent asymmetry by only adjusting the gain of existing coordination patterns in inverse proportion to the amount of target overshoot or undershoot if the movement error was primarily one of extent. Compensating for direction errors would require a more complicated reorganization of coordination patterns, a reorganization that may well take longer to learn.

4. References Cited

Gomi H, Osu R (1998) Task-Dependent Viscoelasticity of Human Multijoint Arm and Its Spatial Characteristics for Interaction with Environments. *J Neurosci* 18: 8965-8978.

Krakauer JW, Pine ZM, Ghilardi M-F, Ghez C (2000) Learning of visuomotor transformations for vectorial planning of reaching trajectories. *J. Neurosci*. 20(23): 8916-8924.

Lacquaniti F, Carrozzo M, Borghese NA (1993) Time-Varying Mechanical Behavior of Multijointed Arm in Man. *J Neurophysiol* 69: 1443-1464.

Perreault EJ, Kirsch RF, Crago, PE (2004) Multijoint dynamics and postural stability of the human arm. *Exp Brain Res* 157: 507-517.

Sainburg RL, Ghilardi MF, Poizner H, Ghez C (1995) Control of limb dynamics in normal subjects and patients without proprioception. *J Neurophysiol* 73(2): 820-835.

Scheidt RA, Conditt MA, Secco EL, Mussa-Ivaldi FA (2005) Interaction of Visual and Proprioceptive Feedback During Adaptation of Human Reaching Movements. *J Neurophysiol* 93: 3200-3213.

Scheidt RA, Ghez C (2007) Separate adaptive mechanisms for controlling trajectory and final position in reaching. *J Neurophysiol* 98: 3600-3613.

Shadmehr R, Mussa-Ivaldi FA (1994) Adaptive representation of dynamics during learning of a motor task. *J. Neurosci* 14: 3208-3224.

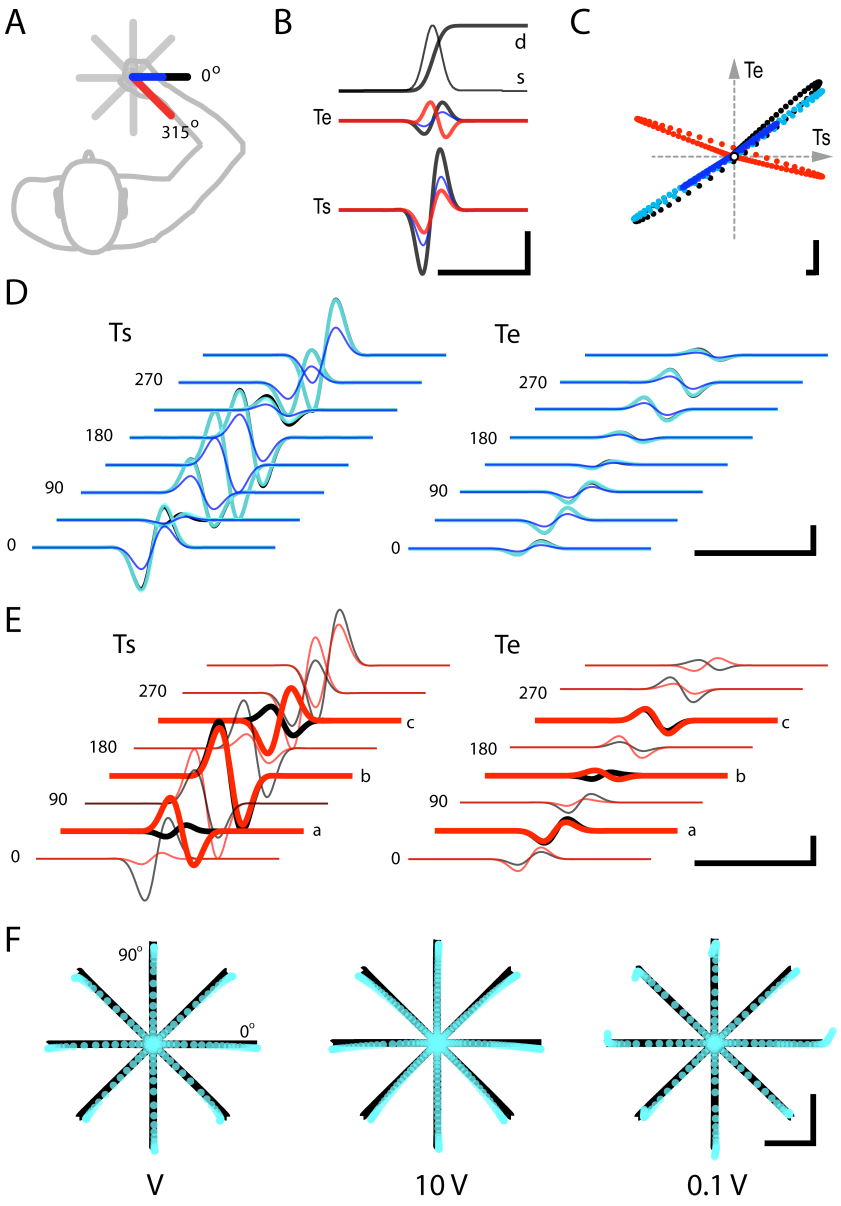

Figure S1: **A**) Movement scenario simulated in this supplemental report. The blue trajectory is half the extent of the black trajectory. **B**) Hand displacement (d) and hand speed profile (s) for the 0° movement shown in panel A. The elbow (Te) and shoulder torques (Ts) for the three highlighted trajectories in panel A are also shown. Color coding as in panel A. Vertical scale: 2.5 Nm; horizontal scale: 0.5 s. **C**) Inter-joint coordination as revealed by plotting Te vs. Ts. Color coding as in panel A. The light blue trace is a scaled (x2) version of the dark blue trace. Vertical and horizontal scales both represent 1 Nm. **D**) Comparison of shoulder (left) and elbow torques (right) estimated from each of the baseline (black) and short (dark blue) template movements. The light blue traces are scaled (x2) versions of the dark blue traces and they closely approximate the black traces for each movement direction at both joints. (In some cases, the black traces are completely hidden by the light blue traces.) Scale bars as in panel B. **E**) Comparison of shoulder (left) and elbow torques (right) estimated from each of the baseline (black) and rotated (red) template movements. Note that there is no simple scaling or staggering of joint torques that could transform the red traces into the black traces across movement directions and joints. Scale bars as in panel B. **F**) Light blue traces correspond to forward dynamics simulations of 10 cm reaches driven by scaled (x2) versions of the torques estimated from the shorter template movements. Black traces represent simulations of 10 cm reaches driven by torques derived from the baseline templates. Terminal accuracy is degraded only slightly if baseline torques are instead approximated by applying a direction-independent scaling rule to joint torques suited for a different movement extent, but in the same movement direction. The results are generally insensitive to the particular choice of V used in the inverse- and forward-dynamic computations. See supplemental text for details. Scale bars: 0.05 m.